Deformation Energy of a Charged Drop. II. Symmetric Saddle Point Shapes

W. J. SWIATECKI*
Institute for Mechanics and Mathematical Physics and The Gustaf Werner Institute for Nuclear Chemistry, Uppsala, Sweden
(Received January 13, 1956)

Symmetric saddle point shapes and threshold energies of a uniformly charged drop are studied for values of the fissionability parameter x in the range 0.6 to 1.0. The method used is a modification of a conventional expansion about a prolate ellipsoid of revolution, which provides some control over the reliability of the approximations made. The electronic machine calculations of Frankel and Metropolis for $x=0.9$, 0.81, 0.77, and 0.74 are consistent with the present work, but their result at $x=0.65$ would appear to be in error.

The calculations with an ellipsoid are preceded by a summary of formulas referring to expansions about a sphere.

1. INTRODUCTION

IN part I[1] certain qualitative features of the deformation energy of a charged drop were considered. In the present paper we shall present quantitative results concerning the threshold energies and symmetric saddle point shapes[2] of incompressible, uniformly charged drops possessing a sharp surface. Such calculations have been made in the past, among others, by Bohr and Wheeler,[2] Present and Knipp,[3] Frankel and Metropolis[4] and, more recently, by Businaro and Gallone[5,6] and Nossoff.[7]

The problem of calculating the surface and electrostatic energies of a strongly deformed drop, though straightforward, involves a considerable amount of labor and, as a rule, approximations have to be introduced. In this respect the present calculations are no exception, but, by using a certain modification of standard methods, it was found possible to throw some light on the difficult question of the validity of the approximations made. As will appear, this turns out to be of some importance for the question of the reliability of some of the calculations referred to above.

The saddle point shapes studied in this paper refer to charged drops with the fissionability parameter x (equal to the electrostatic energy of the spherical configuration over twice the surface energy) in the range 0.6 to 1.0. They are shapes possessing axial and reflection symmetry and tending to the spherical configuration for $x\rightarrow 1$. In the next section we shall consider the case $1-x\ll 1$, for which an expansion about the spherical shape is possible. All the results of that section can be deduced from the existing literature, but, in view of the absence of a comprehensive summary on the one hand, and, on the other, of differences in notation and one or two misprints in the published formulas, we shall begin by collecting the equations relevant to the calculation of electrostatic and surface energies of a slightly distorted drop.

2. SMALL DISTORTIONS OF A SPHERICAL DROP

The equation of the surface of the distorted drop, assumed axially symmetric, may be specified in spherical polar coordinates by

$$R(\theta)=\lambda^{-1}R_0[1+\sum_{n=1}^{\infty}\alpha_n P_n(\cos\theta)], \tag{1}$$

or by

$$R(\theta)=R_0[1+\sum_{n=0}^{\infty}a_n P_n(\cos\theta)]. \tag{2}$$

If the two alternative expansions are to represent one and the same shape, we must have $1+a_0=\lambda^{-1}$ and, for $n\geq 1$, $\alpha_n=\lambda a_n$.

The constancy of the volume of the drop, assumed incompressible, is ensured by the condition

$$\lambda^3=\frac{1}{2}\int_{-1}^{1}(1+\sum_{n=1}^{\infty}\alpha_n P_n)^3 d(\cos\theta).$$

This gives, without approximation,

$$\lambda^3=1+\sum_{1}^{\infty}\frac{3}{2n+1}\alpha_n{}^2+\tfrac{1}{2}\sum_{p,q,r=1}^{\infty}(pqr)\alpha_p\alpha_q\alpha_r,$$

where

$$(pqr)=\int_{-1}^{1}P_pP_qP_r d(\cos\theta)$$

$$=\left(\frac{2}{p+q+r+1}\right)\left(\frac{1\cdot 3\cdots(p+q-r-1)}{2\cdot 4\cdots(p+q-r)}\right)$$

$$\times\left(\frac{1\cdot 3\cdots(p+r-q-1)}{2\cdot 4\cdots(p+r-q)}\right)\left(\frac{1\cdot 3\cdots(r+q-p-1)}{2\cdot 4\cdots(r+q-p)}\right)$$

$$\times\left(\frac{2\cdot 4\cdots(p+q+r)}{1\cdot 3\cdots(p+q+r-1)}\right).$$

(Consult the work of Hobson,[8] p. 87.)

* Now at the Institute of Physics, University of Aarhus, Denmark.

[1] W. J. Swiatecki, Phys. Rev. **101**, 651 (1956).
[2] N. Bohr and J. A. Wheeler, Phys. Rev. **56**, 426 (1939).
[3] R. D. Present and J. K. Knipp, Phys. Rev. **57**, 751 (1940).
[4] S. Frankel and N. Metropolis, Phys. Rev. **72**, 914 (1947).
[5] U. L. Businaro and S. Gallone, Nuovo cimento **1**, 629 (1955).
[6] U. L. Businaro and S. Gallone, Nuovo cimento **1**, 1277 (1955).
[7] V. G. Nossoff, Report A/CONF.8/P/653 U.S.S.R. from the 1955 Geneva Conference on the Peaceful Uses of Atomic Energy (United Nations, New York, 1956).
[8] E. W. Hobson, *The Theory of Spherical and Ellipsoidal Harmonics* (Cambridge University Press, Cambridge, 1931).

TABLE I. The coefficients $(pqr)=\int_{-1}^{1}P_pP_qP_rd(\cos\theta)$.

(222) =4/35	(448) =980/21 879	(112) =4/15	(352) =20/231
(224) =4/35	(466) =56/2431	(132) =6/35	(354) =40/1001
(244) =40/693	(468) =1008/46 189	(134) =8/63	(552) =20/429
(246) =10/143	(488) =72/4199	(154) =10/99	(554) =4/143
(266) =28/715	(666) =800/46 189	(332) =8/105	(336) =200/3003
(268) =56/1105	(668) =700/46 189	(334) =4/77	(572) =42/715
(288) =48/1615	(688) =1200/96 577		
(444) =36/1001	(888) =980/96 577		
(446) =40/1287			

Some of the more frequently occurring of these coefficients are listed in Table I.

The constancy of the position of the center of mass requires that

$$\int_{-1}^{1}(1+\sum_{n=1}^{\infty}\alpha_nP_n)^4\cos\theta d(\cos\theta)=0,$$

which gives

$$\alpha_1=-9\sum_{n=2}^{\infty}\frac{n+1}{(2n+1)(2n+3)}\alpha_n\alpha_{n+1}+\text{terms of order }\alpha_k\alpha_m\alpha_n. \quad (3)$$

The surface and electrostatic energies of the deformed drop, E_s and E_c, in units of their values for a sphere, $E_s^{(0)}$ and $E_c^{(0)}$, can be shown to be given by

$$B_s\equiv\frac{E_s}{E_s^{(0)}}=1+(2/5)\alpha_2^2-(4/105)\alpha_2^3-(66/175)\alpha_2^4-(4/35)\alpha_2^2\alpha_4+\alpha_4^2+(5/7)\alpha_3^2-(8/105)\alpha_2\alpha_3^2-(156/77)\alpha_2^2\alpha_3^2$$
$$-(4/77)\alpha_4\alpha_3^2-(40/231)\alpha_2\alpha_3\alpha_5+(14/11)\alpha_5^2-(12/35)\alpha_1\alpha_2\alpha_3-(4/15)\alpha_1^2\alpha_2-(68/105)\alpha_1^2\alpha_2^2$$
$$-(20/429)\alpha_2\alpha_5^2-(2976/1001)\alpha_2^2\alpha_5^2-(4/143)\alpha_4\alpha_5^2-(36/35)\alpha_1\alpha_2^2\alpha_3-(16/63)\alpha_1\alpha_3\alpha_4+(72/77)\alpha_1\alpha_2^2\alpha_5$$
$$-(20/99)\alpha_1\alpha_4\alpha_5-(324/1001)\alpha_2^2\alpha_3\alpha_5-(80/1001)\alpha_3\alpha_4\alpha_5+\cdots, \quad (4)$$

and

$$B_c\equiv\frac{E_c}{E_c^{(0)}}=1-(1/5)\alpha_2^2-(4/105)\alpha_2^3+(51/245)\alpha_2^4-(6/35)\alpha_2^2\alpha_4-(5/27)\alpha_4^2-(10/49)\alpha_3^2-(92/735)\alpha_2\alpha_3^2$$
$$+(47522/88935)\alpha_2^2\alpha_3^2-(60/539)\alpha_4\alpha_3^2-(5960/17787)\alpha_2\alpha_3\alpha_5-(20/121)\alpha_5^2-(48/245)\alpha_1\alpha_2\alpha_3$$
$$+(2/15)\alpha_1^2\alpha_2+(442/735)\alpha_1^2\alpha_2^2+\cdots. \quad (5)$$

In the above formulas, only some of the more important coefficients in the infinite expansions have been retained. The scale factor λ, given by the next formula, has been taken into account:

$$\lambda^3=1+(3/5)\alpha_2^2+(2/35)\alpha_2^3+0\times\alpha_2^4+(6/35)\alpha_2^2\alpha_4+(1/3)\alpha_4^2+(3/7)\alpha_3^2+(4/35)\alpha_2\alpha_3^2+0\times\alpha_2^2\alpha_3^2$$
$$+(6/77)\alpha_4\alpha_3^2+(20/77)\alpha_2\alpha_3\alpha_5+(3/11)\alpha_5^2+(18/35)\alpha_1\alpha_2\alpha_3+\alpha_1^2+(2/5)\alpha_1^2\alpha_2+(10/143)\alpha_2\alpha_5^2$$
$$+(6/143)\alpha_4\alpha_5^2+(8/21)\alpha_1\alpha_3\alpha_4+(10/33)\alpha_1\alpha_4\alpha_5+(120/1001)\alpha_3\alpha_4\alpha_5\cdots.$$

If the coefficient α_1 is eliminated by means of Eq. (3) [$\alpha_1=-(27/35)\alpha_2\alpha_3+\cdots$] and, in addition, we use $\alpha_n=\lambda a_n$, the following formulas result:

$$B_s=1+(2/5)a_2^2-(4/105)a_2^3-(38/175)a_2^4-(4/35)a_2^2a_4+a_4^2$$
$$+a_3^2[(5/7)-(8/105)a_2-(18346/13475)a_2^2-(4/77)a_4]-(40/231)a_2a_3a_5+(14/11)a_5^2+\cdots, \quad (5a)$$

and

$$B_c=1-(1/5)a_2^2-(4/105)a_2^3+(157/1225)a_2^4-(6/35)a_2^2a_4-(5/27)a_4^2+a_3^2[-(10/49)-(92/735)a_2$$
$$+(1701748/3112725)a_2^2-(60/539)a_4]-(5960/17787)a_2a_3a_5-(20/121)a_5^2+\cdots. \quad (5b)$$

Again only certain terms have been retained. These expressions agree with reference 3.

Recently Nossoff[7] has given formulas for B_c and B_s which enable one to write down all the terms up to order $a_pa_qa_ra_s$. For the sake of completeness we reproduce here Nossoff's formulas in the notation of Eq. (2):

$$B_s=1+\tfrac{1}{2}\sum_{n=2}^{\infty}\frac{(n-1)(n+2)}{2n+1}a_n^2-\tfrac{1}{3}\sum_{l,m,n=2}^{\infty}(lmn)a_la_ma_n+\sum_{m,n=2}^{\infty}\frac{a_n^2a_m^2}{(2n+1)(2m+1)}$$
$$+36\sum_{m,n=2}^{\infty}\frac{(m+1)(n+1)}{(2m+1)(2m+3)(2n+1)(2n+3)}a_ma_{m+1}a_na_{n+1}-(1/128)\sum_{k,l,m,n=2}^{\infty}[k(k+1)+l(l+1)-i(i+1)]$$
$$\times[m(m+1)+n(n+1)-i(i+1)]\cdot(2i+1)(ikl)(imn)a_ka_la_ma_n,$$

and

$$B_c=1-5\sum_{n=2}^{\infty}\frac{n-1}{(2n+1)^2}a_n^2-(5/12)\sum_{l,m,n=2}^{\infty}\frac{7n-10}{2n+1}(lmn)a_la_ma_n+5\sum_{m,n=2}^{\infty}\frac{n-4}{(2n+1)^2(2m+1)}a_n^2a_m^2$$
$$+45\sum_{m,n=2}^{\infty}\frac{(4n-7)(n+1)(m+1)}{(2m+1)(2m+3)(2n+1)^2(2n+3)}a_ma_{m+1}a_na_{n+1}+\tfrac{15}{16}\sum_{\substack{k,l,m,n=2\\ i=0}}^{\infty}\Big\{[i(i+1)-m(m+1)+\tfrac{1}{3}(n^2-n+1)]$$
$$\times\frac{2i+1}{2n+1}+(2/9)[2m(m+1)-(9/4)i(i+1)+n(n+1)](2i+1)-\tfrac{1}{2}(i-1)(i+2)\Big\}(ikl)(imn)a_ka_la_ma_n.$$

The coefficients a_0 and a_1, which do not appear, have been eliminated by means of the constant volume and center-of-mass conditions.

Nossoff's formulas were found to reproduce Eqs. (5a) and (5b) except for the coefficient of $a_3^2a_2^2$ in B_c, which we find would be given as 1 437 121/3 122 725 instead of the 1 701 748/3 112 725 in Eq. (5b). The reason for the discrepancy has not yet been cleared up, but if it is Nossoff's formula which is incorrect, then there is evidence that the mistake may be in the fourth-order term with $a_ma_{m+1}a_na_{n+1}$.

The distortion energy of the drop (surface plus electrostatic energies), in units of $E_s^{(0)}$, is given by

$$\xi=(E_s-E_s^{(0)}+E_c-E_c^{(0)})/E_s^{(0)}$$
$$=(B_s-1)+2x(B_c-1), \quad (6)$$

where $x=E_c^{(0)}/2E_s^{(0)}$.

Using Eqs. (4), (5), and (3), we find

$$\xi=A\alpha_2^2+B\alpha_2^3+C\alpha_2^4+D\alpha_2^2\alpha_4+E\alpha_4^2$$
$$+\alpha_3^2(F+G\alpha_2+H\alpha_2^2+I\alpha_4)+J\alpha_2\alpha_3\alpha_5+L\alpha_5^2+\cdots \quad (7)$$

where the coefficients A to L (linear functions of x) are listed in Table II.

In Eq. (7) all terms with α_n with $n>5$ have been omitted. The reason for the particular selection from among the remaining terms will appear presently.

To determine the saddle point shape which makes ξ in Eq. (7) stationary, we first use

$$\partial\xi/\partial\alpha_4=0 \quad \text{and} \quad \partial\xi/\partial\alpha_5=0,$$

which gives

$$\alpha_4=-(D/2E)\alpha_2^2 \quad \text{and} \quad \alpha_5=-(J/2L)\alpha_2\alpha_3. \quad (8)$$

This leads to an expression for ξ which is a function of α_2 and α_3 only (compare part I):

$$\xi=f(\alpha_2)+\alpha_3^2g(\alpha_2), \quad (9)$$

where

$$f(\alpha_2)=A\alpha_2^2+B\alpha_2^3+\bar{C}\alpha_2^4,$$
$$g(\alpha_2)=F+G\alpha_2+\bar{H}\alpha_2^4, \quad (10)$$

and

$$\bar{C}=C-(D^2/4E),$$
$$\bar{H}=H-(ID/2E)-(J^2/4L).$$

Putting $\alpha_3=0$, the condition $\partial\xi/\partial\alpha_2=0$ gives $\alpha_2^{\text{S.P.}}$ for the symmetric saddle point shape, and substitution in Eq. (9) gives the corresponding threshold energy ξ_{th}. If the term with $\bar{C}$ is neglected, we find, to lowest order in $(1-x)$:

$$\alpha_2^{\text{S.P.}}=-2A/3B=(7/3)(1-x),$$
$$\xi_{\text{th}}=(4/27)(A^3/B^2)=(98/135)(1-x)^3. \quad (11)$$

The inclusion of $\bar{C}$ gives instead:

$$\alpha_2^{\text{S.P.}}=2.3333(1-x)-1.2261(1-x)^2,$$
$$\alpha_4^{\text{S.P.}}=(168/85)(1-x)^2, \quad (12)$$
$$\xi_{\text{th}}=0.7259(1-x)^3-0.3302(1-x)^4.$$

The function $g(\alpha_2)$ in Eq. (9) is a measure of the stability of the symmetric shapes against asymmetry. The symmetric shape in question is that specified by α_2 and α_4 [$\alpha_4=-(D/2E)\alpha_2^2$], and the asymmetric distortion contemplated is given by α_3 and α_5[$\alpha_5=-(J/2L)\alpha_2\alpha_3$)]. Inserting into Eq. (10) the expression for $\alpha_2^{\text{S.P.}}$ from Eq. (12), we find the following expansion for $g(\alpha_2^{\text{S.P.}})$, which now measures the stability of saddle point shapes against the most favorable

TABLE II. Coefficients in the expansion of the deformation energy ξ.

Term		Fractions
A	α_2^2	$\frac{2}{5}-\frac{2}{5}x$
B	α_2^3	$-\frac{4}{3\cdot5\cdot7}-\frac{8}{3\cdot5\cdot7}x$
C	α_2^4	$-\frac{66}{5\cdot5\cdot7}+\frac{102}{5\cdot7\cdot7}x$
D	$\alpha_2^2\alpha_4$	$-\frac{4}{5\cdot7}-\frac{12}{5\cdot7}x$
E	α_4^2	$1-\frac{10}{3\cdot3\cdot3}x$
F	α_3^2	$\frac{5}{7}-\frac{20}{7\cdot7}x$
G	$\alpha_2\alpha_3^2$	$-\frac{8}{3\cdot5\cdot7}-\frac{184}{3\cdot5\cdot7\cdot7}x$
H	$\alpha_2^2\alpha_3^2$	$-\frac{23736}{5\cdot5\cdot7\cdot7\cdot11}+\frac{4267436}{3\cdot5\cdot5\cdot7\cdot7\cdot7\cdot11\cdot11}x$
I	$\alpha_4\alpha_3^2$	$-\frac{4}{7\cdot11}-\frac{120}{7\cdot7\cdot11}x$
J	$\alpha_2\alpha_5\alpha_3$	$-\frac{40}{3\cdot7\cdot11}-\frac{11920}{3\cdot7\cdot7\cdot11\cdot11}x$
L	α_5^2	$\frac{14}{11}-\frac{40}{11\cdot11}x$

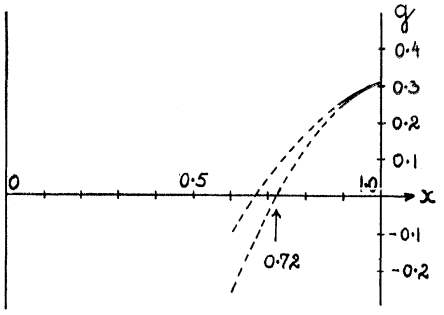

FIG. 1. Stability against asymmetry of saddle point shapes as function of x. The lower curve is $g(\alpha_2^{S.P.})$ from Eq. (13). The calculation is based on an expansion about a sphere and becomes more and more unreliable as x decreases below about 0.9. The intersection with the x axis at $x=0.72$ is, therefore, a very uncertain estimate of the critical x_c at which instability of the symmetric saddle point shape against asymmetry first appears. In particular, a value of x_c considerably lower than 0.72 could not be ruled out by the trend of g for $x \gtrsim 0.9$, the region where the calculation is reliable. The upper curve refers to the case when α_5 is put equal to zero.

asymmetry:

$$g(\alpha_2^{S.P.})=0.3061-0.3571(1-x)-2.7118(1-x)^2, \quad (13)$$

valid for $(1-x)\ll 1$.

The reason for retaining the 11 terms in Eq. (7) is now clear. The lowest order formula for ξ_{th} requires the terms in A and B, whereas the correction in $(1-x)^4$ makes use of C, D, and E. Similarly, F gives the first term in Eq. (13), G is needed for the second, and H, I, J, and L are required for the third term.

If higher even harmonics P_6, P_8, etc., were included in Eq. (1), the coefficients α_6, α_8, etc., would, like α_4, be of order $(1-x)^2$. [Contrast reference 7 which implies that, for $n>1$, α_{2n} is of order $(1-x)^n$. The unique position of α_2, which is of order $(1-x)$, is associated with the fact that P_2 is the special distortion for which stability is lost at $x=1$]. The effect of P_n with $n>4$ on ξ_{th} would, therefore, start with the term in $(1-x)^4$. The coefficient -0.3302 in Eq. (12) is thus only an approximation to the correct term in $(1-x)^4$. The inclusion of the higher even harmonics should always lower the estimate of ξ_{th} for a given x, since, with more degrees of freedom available, the passage over the potential barrier can be made in a more economical way.

Similarly, the inclusion of odd harmonics P_n with $n>5$ would affect the last term in Eq. (13). The effect would be always to decrease g, since there would be greater freedom in choosing the asymmetric distortion most likely to lower the energy. This is illustrated by a comparison of Eq. (13) with an analogous expansion in which, however, the coefficient α_5 is taken as zero instead of that function of α_2 and α_3 which minimizes the energy [Eq. (8)]. The last term in Eq. (13) is then replaced by $-1.6844(1-x)^2$. The two cases are shown in Fig. 1.

Information concerning the range of validity of the formulas discussed so far, considered as functions of $1-x$, will be provided by a comparison with the more exact calculations of the following sections.

3. LARGE DEFORMATIONS

The formulas of the preceding section were derived under the assumption that the deviations from the spherical shape are small, which is not the case in applications to nuclear fission (when values of x around 0.7 are of interest). In reference 4, electronic machine calculations were carried out which, in principle, should be accurate also for large distortions. In this and the following sections, we shall report some results of studies of this problem using analytical methods.

Figure 2(c) compares the saddle point shape for $x=0.699$ with an ellipse whose axes are in the ratio 1:2.4004. In so far as the saddle point shape can be regarded as a small distortion of the ellipse, an expansion of the surface and electrostatic energies in powers of the distortion should be useful. One could proceed in analogy with the case of the distorted sphere and write down E_s and E_c to (at least) the second power of the distortion and, by differentiation, determine the configuration which makes the total energy stationary. (This is the procedure followed in references 6 and 7.) In practice, an alternative method was found to possess several advantages, which turned out to be of decisive importance in making practicable an accurate determination of the thresholds and saddle point shapes. The method makes use of the general equation for the surface of a liquid in equilibrium under the action of a surface tension and of electrostatic forces, *viz.*:

$$v\rho+S\kappa=\text{constant}=k. \quad (14)$$

Here v is the electrostatic potential at a point on the surface of the liquid, κ is the total curvature at that point, ρ is the (uniform) charge density, and S is the constant surface energy per unit area.

The above relation results from equating to zero the first-order change in the total energy associated with a small volume-preserving deformation of the surface. If the deformation is specified by a normal displacement of the surface, δn, then the change in the energy is

$$E=\delta\left(\int_{\text{volume}} \tfrac{1}{2}v\rho+\int_{\text{surface}} S\right)$$

$$=\int_{\text{surface}} v\rho\delta n+\int_{\text{surface}} S\kappa\delta n.$$

Subtracting $\int_{\text{surface}}\delta n$ times a Lagrange multiplier k to ensure conservation of volume and equating to zero the integrand leads to Eq. (14). The Lagrange multiplier k is determined by considering the effect of a uniform change of scale on a shape satisfying Eq. (14). The associated change in the total energy can be

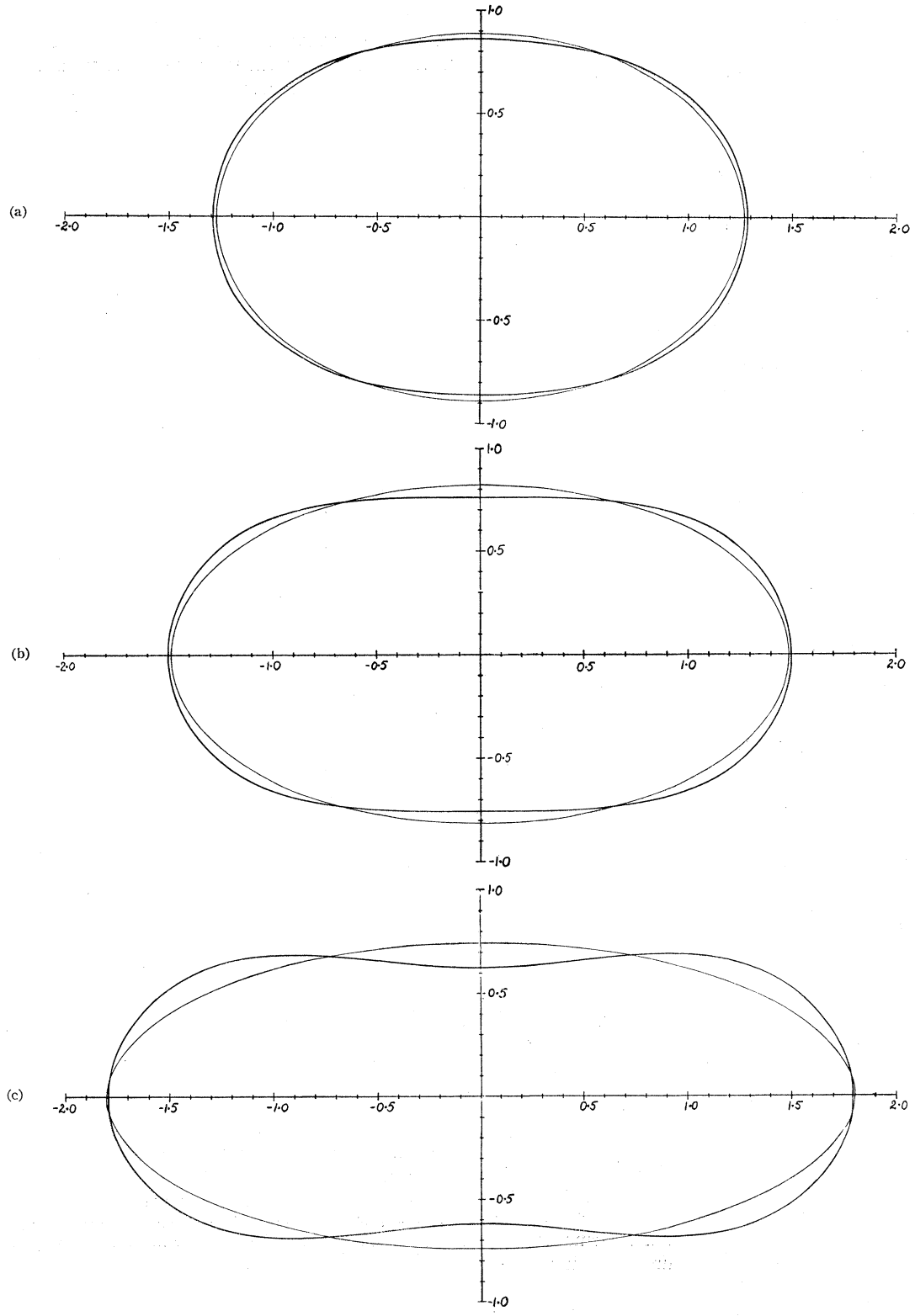

FIG. 2. Three ellipses, given in spheroidal coordinates by $\eta_0=1.4$, 1.2, and 1.1, and the saddle point shapes for $x=0.876$, 0.792, and 0.699. Each of the three sets represents an optimum adjustment of the saddle point shape and the initial ellipse which minimizes the residual in the least squares fit. The values of the expansion coefficients ϵ_n defining the saddle point shapes [Eq. (17)] are as follows: (a) $\epsilon_2=0.03777$, $\epsilon_4=-0.02859$, $\epsilon_6=0.00347$; (b) $\epsilon_2=0.03393$, $\epsilon_4=-0.03693$, $\epsilon_6=0.00687$; (c) $\epsilon_2=0.03040$, $\epsilon_4=-0.04100$, $\epsilon_6=0.01019$.

written in two ways. On the one hand,

$$E=\int_{\text{surface}}(v\rho+S\kappa)\delta n=k\int_{\text{surface}}\delta n=k\delta V,$$

where δn is now the non-volume-preserving displacement of the surface associated with the change of scale and δV is the corresponding volume change. On the other hand, from a dimensional argument,

$$\delta E=\delta E_s+\delta E_c=E_s\left(\frac{V+\delta V}{V}\right)^{\frac{2}{3}}+E_c\left(\frac{V+\delta V}{V}\right)^{5/3}$$

$$-E_s-E_c=[(\tfrac{2}{3})E_s+(5/3)E_c]\left(\frac{\delta V}{V}\right).$$

Hence $k=[(\frac{2}{3})E_s+(5/3)E_c]/V$, where V, E_s, and E_c are the volume, and the surface and electrostatic energies of the equilibrium shape, respectively. Expressing all quantities in units of their values for a spherical configuration, Eq. (14) can be written in the form

$$x\left(\frac{v}{v_0}-B_c\right)+\frac{1}{5}\left(\frac{\kappa}{\kappa_0}-B_s\right)=0, \tag{15}$$

where v_0 and κ_0 are the surface potential and total curvature of the original sphere and B_c and B_s are as defined in Sec. 2.

To determine the distortion of an ellipsoid which will ensure the validity of Eq. (15), one may now write down the surface potential and curvature as functions of position on the surface, expand in powers of the distortion, and satisfy Eq. (15) by, for example, a least-squares fit. The disadvantage, that in this method one has to calculate the expansion of a function of position on the surface of the drop rather than of a number (the total energy) as in the conventional treatment, is offset by several factors. Firstly, since Eq. (15) represents the stage *after* the differentiation of the total energy which determines the equilibrium shape, an approximation equivalent to calculating the energy to second power in the distortion is obtained by writing down v and κ in Eq. (15) only to first power. This avoids the necessity of deriving the complicated formulas for second-order effects. Secondly, if, as is usually done, the distortion of the ellipse is written as a superposition of several harmonic distortions, analogous to $\sum_0^N a_nP_n$ in the case of a sphere, the number of coefficients in the expansion of the energy to second order is proportional to N^2, whereas, using Eq. (15), only one new function has to be calculated for each additional harmonic (see below). Moreover, since one is dealing with first-order formulas, general expressions for any n are readily written down. As will appear presently, this made practicable the inclusion of an adequate number of harmonics and the demonstration of the virtual independence of the results of additional terms. Thirdly, and most important, the last step in the present procedure, the reduction to zero by least squares of a certain expression claimed to be an approximation to $v\rho+S\kappa-k$ on the surface of a distorted ellipsoid (obtained by expanding in powers of the distortion), provides a check for the absence of accidental computational errors as well as for the validity of the assumed expansion. Thus, a computational error will, as a rule, show up in the impossibility of satisfying Eq. (15). Similarly it was found that the expected breaking down of the expansion in powers of the distortion, which results from attempting to use a given ellipse as a starting point for saddle point shapes differing from the ellipse by too great an amount, could be followed quantitatively by a study, as function of x, of the *residual* in the least-squares method. The minimum in the residual corresponds to an optimum adjustment of the starting ellipse and the saddle point shape which it is supposed to approximate. By always working at this optimum, an objective way of picking out the most accurate and reliable solutions was achieved. No corresponding method is available in the conventional approach in which the energy is expanded to second order.

In order to represent the distorted ellipsoids, prolate spheroidal coordinates η, ξ, ϕ were used,[9] related to cylindrical polar coordinates ρ, z, ϕ by

$$\begin{aligned}\rho&=c_2(1-\xi^2)^{\frac{1}{2}}(\eta^2-1)^{\frac{1}{2}},\\ z&=c_2\xi\eta,\end{aligned} \tag{16}$$

where c_2 is a constant. (The above ξ must not be confused with the deformation energy denoted by the same symbol.)

The equation of an ellipse in these coordinates is given by $\eta(\xi)=\text{constant}=\eta_0$ (c_2 is then the z-coordinate of the focus of the ellipse). The coordinates η, ξ, ϕ correspond to r, θ, ϕ in the case of spherical polar coordinates, with ξ specifying the position on the surface of an ellipsoid (defined by $\eta=\text{constant}$) in analogy to θ specifying the position on the surface of a sphere (defined by $r=\text{constant}$).

The equation of an arbitrary axially symmetric surface was usually taken in the form

$$\begin{aligned}\eta&=\eta(\xi)\\ &=\eta_0[1+(\eta_0^2-\xi^2)^{-1}\sum_{n=0}^{\infty}\epsilon_nP_n(\xi)].\end{aligned} \tag{17}$$

Constancy of volume and center of mass is then ensured to first order by $\epsilon_0=\epsilon_1=0$.

The surface potential and curvature [or rather the two parts of Eq. (15)] will, to first order in ϵ_n, have the form: (function of ξ)$+\sum_{n=2}^{\infty}$ (function of ξ)$_n\epsilon_n$, i.e.,

$$\frac{v}{v_0}-B_c=A(\xi)+\sum_{n=2}^{\infty}\epsilon_nA_n(\xi), \tag{18}$$

[9] W. R. Smythe, *Static and Dynamic Electricity* (McGraw-Hill Book Company, Inc., New York, 1939).

with[10]

$$B_c = a + a_2\epsilon_2. \tag{19}$$

Similarly,

$$\frac{1}{5}\left(\frac{\kappa}{\kappa_0} - B_s\right) = B(\xi) + \sum_{n=2}^{\infty} \epsilon_n B_n(\xi), \tag{20}$$

$$B_s = b + \sum_{2}^{\infty} b_n \epsilon_n. \tag{21}$$

Here $A(\xi)$, $A_n(\xi)$, $B(\xi)$, and $B_n(\xi)$ are functions of position on the surface of the ellipsoid. Together with the constants a, a_2, b, b_n they are defined in the Appendix.

By using Eqs. (18) and (20), the condition (15) can be written as

$$f \equiv G(\xi) + \sum_{n=2}^{\infty} \epsilon_n G_n(\xi) = 0, \tag{22}$$

where $G = xA + B$ and $G_n = xA_n + B_n$ are functions of ξ depending linearly on x. The least squares condition, taken in the form

$$\delta \int_{\substack{\text{surface of}\\ \text{ellipsoid}}} f^2 d\sigma = 0,$$

where δ means independent variations of the ϵ_n in f^2, then leads to the following two sets of simultaneous linear equations for the optimum values of ϵ_n specifying an equilibrium shape:

$$\begin{aligned} &(22)\epsilon_2 + (24)\epsilon_4 + (26)\epsilon_6 + \cdots + (2) = 0,\\ &(24)\epsilon_2 + (44)\epsilon_4 + (46)\epsilon_6 + \cdots + (4) = 0,\\ &(26)\epsilon_2 + (46)\epsilon_4 + (66)\epsilon_6 + \cdots + (6) = 0,\\ &\cdots \end{aligned} \tag{23}$$

and

$$\begin{aligned} &(33)\epsilon_3 + (35)\epsilon_5 + \cdots = 0,\\ &(35)\epsilon_3 + (55)\epsilon_5 + \cdots = 0.\\ &\cdots \end{aligned} \tag{24}$$

Here

$$(rs) \propto \int_{\substack{\text{surface of}\\ \text{ellipse}}} G_r G_s d\sigma$$

and

$$(r) \propto \int_{\substack{\text{surface of}\\ \text{ellipse}}} G G_r d\sigma. \tag{25}$$

In practice the functions $G_r(\xi)$ were calculated for eleven values of ξ, at $\xi_i = 0$, 0.15, 0.30, 0.45, 0.60, 0.70, 0.80, 0.85, 0.90, 0.95 and, 1.00 ($i = 1, 2, 3, \cdots 11$) and the integrals in Eq. (25) were replaced by sums. The smaller intervals in ξ_i near $\xi = 1$ are designed to give a better representation near the tips of the ellipse (see below). Because of the symmetry of the integrands in Eq. (25), only positive values of ξ need be considered. [Note that $G(\xi)$ and $G_n(\xi)$ with n even are even functions of ξ, and $G_n(\xi)$ with n odd are odd functions.] Explicitly, the sums for (rs) and (r) were taken as

$$\begin{aligned} (rs) &= \sum_{i=1}^{11} G_r(i) G_s(i) (\eta_0^2 - \xi_i^2)^{\frac{1}{2}} \Delta\xi_i,\\ (r) &= \sum_{i=1}^{11} G(i) G_r(i) (\eta_0^2 - \xi_i^2)^{\frac{1}{2}} \Delta\xi_i. \end{aligned} \tag{26}$$

The factor $(\eta_0^2 - \xi_i^2)^{\frac{1}{2}}\Delta\xi_i$ is proportional to the surface element $d\sigma$ associated with ξ_i. [Thus $\Delta\xi_i = 0.075$, 0.15, 0.15, 0.15, 0.125, 0.1, 0.075, 0.05, 0.05, 0.05, 0.025 for $i = 1, 2, \cdots 11$. The factor $(\eta_0^2 - \xi_i^2)^{\frac{1}{2}}$ represents the result of integrating over the azimuth ϕ.]

The solution of Eqs. (23) gives the symmetric saddle point shape, specified by a set of $\epsilon_n{}^{\text{S.P.}}$. The threshold energy follows from using Eqs. (6), (19), and (21). Note that Eqs. (19) and (21) give only the linear terms in ξ considered as function of ϵ_n. The derivation of the quadratic terms in B_c and B_s can be avoided by remembering that the value of a quadratic expression $y = a + bx + cx^2$, calculated at the point x_1 where the first derivative y' vanishes, is given by $y(x_1) = a + b(x_1/2)$, which does not require a knowledge of c. Hence, with the values of $\epsilon_n{}^{\text{S.P.}}$ available, the threshold energy is given by Eq. (6), but with B_s and B_c in Eqs. (19) and (21) evaluated at $\epsilon_n = \frac{1}{2}\epsilon_n{}^{\text{S.P.}}$.

The other set of simultaneous linear equations, Eqs. (24), is always satisfied by $\epsilon_{n\ \text{odd}} = 0$, corresponding to symmetric shapes. If, however, the determinant of the coefficients in Eq. (24) should happen to vanish, the set of equations can also be satisfied by finite values of $\epsilon_{n\ \text{odd}}$. This corresponds to the appearance of asymmetric saddle point shapes. (See part I.) Asymmetric shapes will not, however, be discussed further in the present paper.

4. RESULTS

Calculations were carried out with three different ellipses as starting points, specified by $\eta_0 = 1.4$, 1.2, and 1.1. The ratios of the major axis to the minor axis, given by $(1-\eta_0^2)^{-\frac{1}{2}}$, are 1.4289, 1.8091, and 2.4004, respectively. The ellipses are shown in Figs. 2(a), 2(b), and 2(c). Up to 4 even harmonics ϵ_2, ϵ_4, ϵ_6, and ϵ_8 were used in the expansion (17), but the term in ϵ_8 was found to have a negligible effect and was later omitted. With any given η_0, saddle point shapes were calculated for a range of values of x. [The calculations of (rs) and (r) for several values of x are simplified if one notes that these coefficients are quadratic functions of x.] Each solution was checked by plotting $f = G(\xi) + \sum_{n=2}\epsilon_n G_n(\xi)$ as function of ξ. With all ϵ_n put equal to zero, the quantity $f_0 = G(\xi)$ is equal to $x[(v/v_0) - B_c] + \frac{1}{5}[(\kappa/\kappa_0) - B_s]$ evaluated on the surface of an undistorted ellipse. The deviation of f_0 from zero, for example its root-mean-square value, is a measure of the inadequacy of an

[10] For the reason why coefficients a_n with $n > 2$ do not appear in (19), see Appendix.

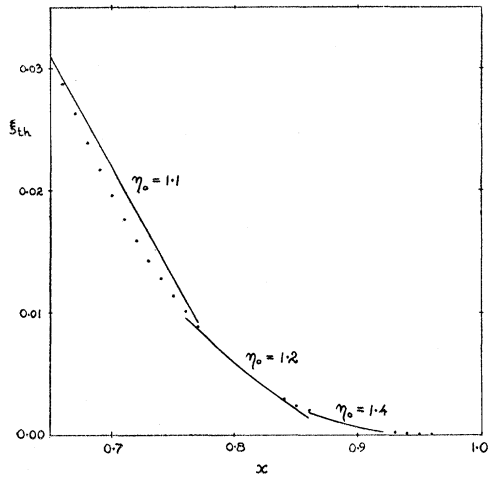

FIG. 3. The thresholds ξ_{th}, calculated using the starting point ellipsoids $\eta_0=1.1$, 1.2, and 1.4. For each ellipsoid a range of values of x was investigated (reaching beyond the range of validity of the expansions used) and the results are shown by the three curves in the figure. The dots represent the trend of the lowest order formula $\xi_{\text{th}}=0.726(1-x)^3$.

ellipse as a representation of a saddle point shape. The rms value of f is similarly a measure of the residual deviations for the deformed ellipse. We have used the ratio

$$\chi=\left\{\frac{\sum_{i=1}^{11}\left[G(i)+\sum_{n=2}^{6}G_n(i)\epsilon_n{}^{\text{S.P.}}\right]^2(\eta_0^2-\xi_i^2)^{\frac{1}{2}}\Delta\xi_i}{\sum_{i=1}^{11}\left[G(i)\right]^2(\eta_0^2-\xi_i^2)^{\frac{1}{2}}\Delta\xi_i}\right\}^{\frac{1}{2}}$$

as a measure of the relative accuracy of the method for a given η_0 and different values of x. (The main variation of χ with x comes from the numerator.)

The result of the threshold energy calculations is shown in Fig. 3. The rapid increase of ξ_{th} with $(1-x)$ [for $1-x\ll 1$, $\xi_{\text{th}}\propto(1-x)^3$] is seen to continue down to $x\sim 0.65$. It will be noted that the calculations with $\eta_0=1.1$, 1.2, and 1.4 do not give identical results in the regions where the x values investigated with the three different starting point ellipses overlap. This is to be expected, since an expansion about one of the ellipses will be approximately valid only in the neighborhood of a certain x. As one goes away from this neighborhood the results will become more and more inaccurate. This can be seen more clearly in Fig. 4, where ξ_{th}, divided by $(1-x)^3$, has been plotted. As mentioned above, the breaking down of the expansions is apparent also in a study of the residuals $f(\xi)$ or the ratios χ (the latter plotted in the upper part of Fig. 4). Two typical cases are analyzed in detail in Figs. 5(a) and 5(b), corresponding to calculations with $x=0.699$ and $x=0.74$, respectively (both using the ellipse $\eta_0=1.1$). The residual $f(\xi)$ in Fig. 5(a) is such that χ is only $2\frac{1}{2}\%$, and part of the remaining rapid oscillation in $f(\xi)$ would, presumably, be removed by introducing $\epsilon_8 P_8$ and higher harmonics in the expansions. On the other hand in Fig. 5(b), the residual χ is $8\frac{1}{2}\%$ and the long period deviation of $f(\xi)$ from zero was found to be practically unaffected by the introduction of $\epsilon_8 P_8$, and must be taken as an indication of the breaking down of the expansions.

It so happened that the initial applications of the present method were made precisely with $x=0.74$. The reason for the residual deviation of $f(\xi)$ from zero was, at that time, not clear, and considerable effort went into searching for suspected errors, thereby checking the correctness of all formulas. A by-product of the search was the localization on the surface of the ellipsoid of the region where the greatest inaccuracy in the expansion (22) arises. It was found, namely, that if (with $x=0.74$) the least squares condition is relaxed by leaving out, in turn, the points at $\xi_i=1.0$, 0.95, 0.90, 0.85, and 0.80, then at first the nature of the solution changes rather rapidly and the residual $f(\xi)$ over the remaining region of ξ values decreases quickly. With $\xi_i=1.0$, 0.95, and 0.90 left out, however, the residual is practically zero and the neglect of further points has a small effect. This was taken as a confirmation of an impres-

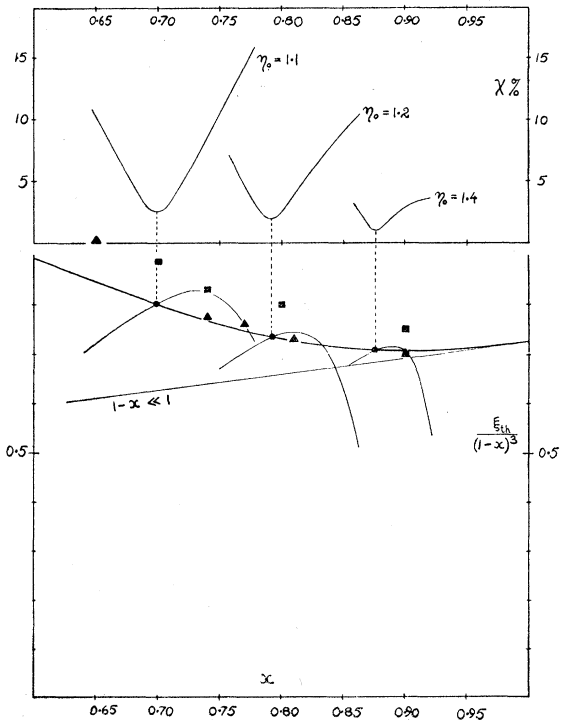

FIG. 4. The lower part of the figure shows the values of $\xi_{\text{th}}/(1-x)^3$, calculated using the three ellipsoids $\eta_0=1.1$, 1.2, and 1.4. In the upper part the residuals χ in the least squares method are plotted against x. The minima in χ pick out the most reliable solutions. The corresponding values of $\xi_{\text{th}}/(1-x)^3$ are shown circled and the interpolation-extrapolation curve (27), passing through these points is shown by the thicker line. The results of the electronic machine calculations of Frankel and Metropolis[4] are indicated by triangles and those of Businaro and Gallone[6] by squares.

sion, formed on more indirect evidence, that the greatest error in the expansion occurs near the tips of the ellipsoid. Note that the large value of f_0 for $\xi>0.9$ (Fig. 5) suggests the relative poorness of the ellipse as a representation of the saddle-point shape in that region.

In the same connection it was found that the eleven points ξ_i on the surface of the ellipsoid were sufficiently closely spaced to make the results virtually independent of taking a finer subdivision in the summations over i. Thus, the inclusion of four additional points at $\xi_i=0.88$, 0.93, 0.97, and 0.99 had a negligible effect on the solution.

The minima in the curves for χ in Fig. 4 pick out the most reliable sets of calculations at the three optimum x values, $x=0.699$, 0.792, and 0.876, associated with the ellipses $\eta_0=1.1$, 1.2, and 1.4, respectively. The corresponding values of $\xi_{\text{th}}/(1-x)^3$ are 0.800, 0.733, and 0.707, and the residual rms values of $f(\xi)$ are 2.5%, 1.8%, and 0.9% of their values for the undistorted ellipses.

The relatively accurate solutions at the above values of x may be used, together with the limiting solution for $1-x\ll 1$, to construct an interpolation-extrapolation formula for ξ_{th}. The expression

$$\xi_{\text{th}}=(1-x)^3[0.7259-0.3302(1-x)+0.6387(1-x)^2 +7.8727(1-x)^3-12.0061(1-x)^4] \quad (27)$$

passes through the three calculated points and has the correct behavior for $x\to 1$. The above function is tabulated at intervals of 0.01 in Table III, for x values in the range 0.6 to 1.0. A plot is given in Fig. 6, where the limiting behavior for $x\ll 1$ is also shown.[2] A further

TABLE III. The threshold energy ξ_{th} and $\xi_{\text{th}}/(1-x)^3$, as functions of x. [Based on formulas (27) and (28).]

x	ξ_{th}	$\xi_{\text{th}}/(1-x)^3$	x	ξ_{th}	$\xi_{\text{th}}/(1-x)^3$
1.00	0.0	0.7259	0.73	0.01524	0.7745
0.99	0.0^67227	0.7227	0.72	0.01718	0.7825
0.98	0.0^55757	0.7196	0.71	0.01929	0.7909
0.97	0.0^41935	0.7168	0.70	0.02159	0.7996
0.96	0.0^44571	0.7142	0.69	0.02409	0.8086
0.95	0.0^48899	0.7119	0.68	0.02679	0.8177
0.94	0.0001533	0.7099	0.67	0.02972	0.8270
0.93	0.0002429	0.7083	0.66	0.03288	0.8365
0.92	0.0003620	0.7071	0.65	0.03627	0.8459
0.91	0.0005149	0.7063	0.64	0.03991	0.8555
0.90	0.0007059	0.7059	0.63	0.04381	0.8649
0.89	0.0009397	0.7060	0.62	0.04797	0.8743
0.88	0.001221	0.7066	0.61	0.05241	0.8835
0.87	0.001555	0.7076	0.60	0.05712	0.8925
0.86	0.001946	0.7092			
0.85	0.002400	0.7112	0.55	0.08070	0.886
0.84	0.002924	0.7138	0.50	0.1029	0.823
0.83	0.003522	0.7169	0.45	0.1237	0.744
0.82	0.004202	0.7205	0.40	0.1433	0.663
0.81	0.004970	0.7246	0.35	0.1616	0.588
0.80	0.005834	0.7292	0.30	0.1788	0.521
0.79	0.006800	0.7343	0.25	0.1948	0.462
0.78	0.007878	0.7399	0.20	0.2098	0.410
0.77	0.009075	0.7459	0.15	0.2237	0.364
0.76	0.01040	0.7524	0.10	0.2367	0.325
0.75	0.01187	0.7594	0.05	0.2487	0.290
0.74	0.01348	0.7667	0.00	0.2599	0.260

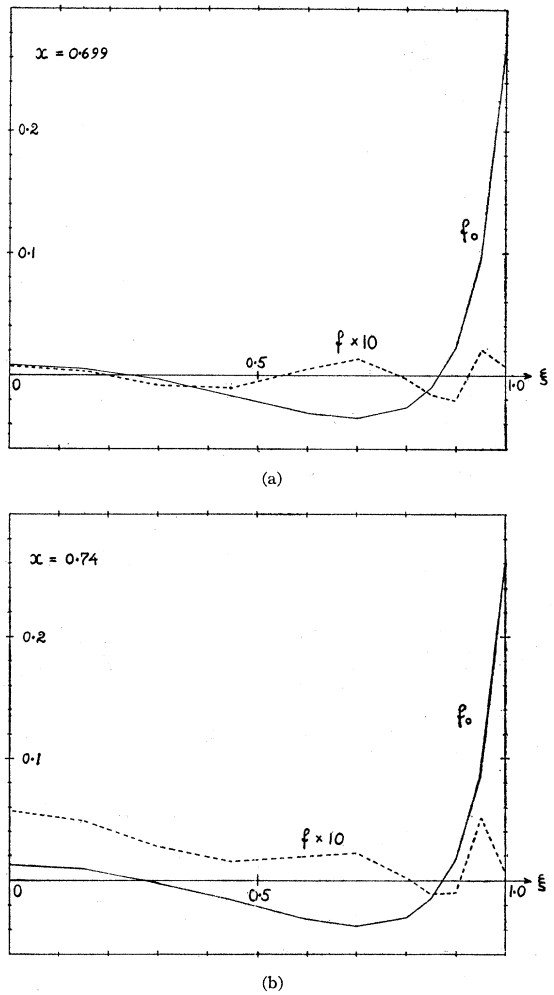

FIG. 5. (a) The curve f_0 is the quantity $x[(v/v)_0-B_c)]+[\frac{1}{5}(\kappa/\kappa_0)-B_s]$, (with $x=0.699$), plotted as function of position on the surface of the ellipsoid $\eta_0=1.1$. This quantity would be zero for a saddle point shape. The dotted curve f is (ten times) the same quantity for a distorted ellipsoid representing an approximation to the saddle point shape. The rms value of f divided by the rms value of f_0 is $\chi=2\frac{1}{2}\%$. (b) Same as Fig. 5(a) but for $x=0.74$. The value of χ is $8\frac{1}{2}\%$.

interpolation formula which has the correct behavior at $x\ll 1$ and which, at $x=0.6$ is equal in value and first derivative to ξ_{th} from Eq. (27), is provided by

$$\xi_{\text{th}}=0.2599-0.2151x-0.1643x^2-0.0673x^3. \quad (28)$$

This function is also plotted in Fig. 6 (dashed line) and tabulated, in the range $x=0$ to $x=0.6$, in Table III. It should be stressed, however, that the behavior of ξ_{th} in the range $x=0.1$ to 0.6 is not well defined by the available calculations, and the use of Eq. (28) is no better than a free-hand interpolation.

If, in addition to ξ_{th}, the values of B_c and B_s for the saddle point shapes are required separately, one may first determine B_c from the general relation

$$d\xi_{\text{th}}/dx=2(B_c-1), \quad (29)$$

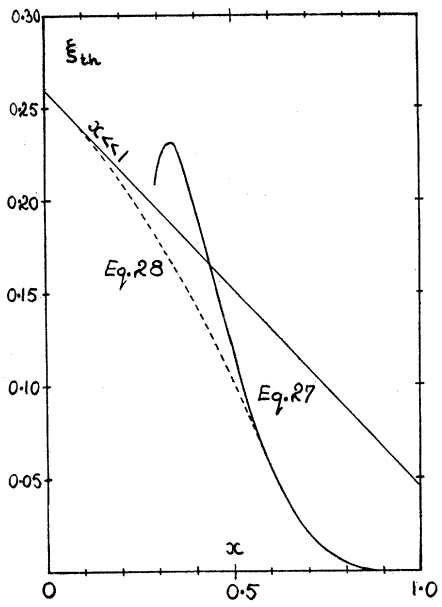

FIG. 6. The threshold ξ_{th} in the range $x=0$ to $x=1$. The interpolation-extrapolation formula (27), applicable for x greater than about 0.6, is plotted beyond its range of validity. The behavior of ξ_{th} for $x \ll 1$ is indicated by the straight line. The interpolation formula (28) (dashed line), which has the correct value and slope at $x=0$ and $x=0.6$, suggests how the intermediate region might be spanned.

obtained by differentiating Eq. (6). {The total variation $\delta\xi_{th}$ in Eq. (6) is the sum of a term coming from varying x at a constant shape of the drop [Eq. (29)] and a term coming from varying the shape at a constant x. The latter term is zero on account of the stationary nature of the energy at a saddle point.}

Using Eq. (27), one finds

$$B_c=1-(1-x)^2[1.0889-0.6604(1-x)+1.5968(1-x)^2+23.6181(1-x)^3-42.0214(1-x)^4].$$

With B_c and ξ_{th} available, B_s can be found from Eq. (6).

The saddle point shapes corresponding to the three optimum solutions on which the above formulas are based are shown in Figs. 2(a), 2(b), and 2(c), together with the undistorted ellipses. It may be noted that for these shapes the second and fourth harmonics ξ_2 and ξ_4 are about equally important (with the second tending to predominate for higher x and the fourth for lower x values). The sixth harmonic ϵ_6 is smaller, though still not negligible, especially for the lower x values. The eight harmonic ϵ_8, however, was found to be very small. Even with the ellipse $\eta_0=1.1$, where the higher harmonics are more in evidence, the values of ϵ_8 did not exceed a few units in the fourth decimal place. For example, at $x=0.7$, $\epsilon_8=0.0004$. The contribution of such a term to ξ_{th} is then 0.000017 or 0.08%.

The saddle point shapes for the three optimum x values can again be used to deduce saddle point shapes for other x values by interpolation and extrapolation. This was done graphically by reading off the radius vectors $R(\theta)$ of the three optimum shapes at intervals of 10°, plotting these against x, and drawing smooth curves with the correct behavior near $x\rightarrow 1$ [as determined by $R(\theta)=R_0(1+\alpha_2 P_2)$, with $\alpha_2=(7/3)(1-x)$]. The result is shown in Fig. 7, where the limiting values for $x=0$ are also shown.[2] The curves in Fig. 7 were used to construct the five saddle point shapes at $x=1.0$, 0.9, 0.8, 0.7, 0.6 shown in Fig. 8. The extrapolation to $x=0.6$ might be inaccurate by a noticeable amount. The corresponding radius vectors are given in Table IV.

The threshold energies calculated in this paper are compared with the results of other authors in Fig. 4. With one exception, the electronic machine calculations of Frankel and Metropolis[4] are consistent with our results. Thus, at $x=0.74$, where, in the words of the authors "the most accurate and extensive calculations were made," the value of ξ is given as 0.013_6, to be compared with our $\xi=0.0135$. At $x=0.9$, Frankel and Metropolis find $\xi=0.0007$ as against our $\xi=0.000706$, and at $x=0.81$, $\xi=0.0050$ against our 0.00497. The threshold at $x=0.77$ "was investigated briefly" by Frankel and Metropolis. The value $\xi=0.009_3$ is consistent with our 0.00908. At $x=0.65$, however, the electronic machine calculations gave $\xi=0.0400$ against our $\xi=0.0363$. The discrepancy is even more apparent in the corresponding saddle point shape which, according to Frankel and Metropolis, has at this value of x separated into two almost distinct fragments, connected by a narrow neck. That there must be some error in those calculations is suggested by a simple estimate which indicates that the diameter of the neck is several times to small for the surface tension round its perimeter to balance the still considerable electrostatic repulsion between the two halves of the drop. This shows that the shape is not in equilibrium and cannot, therefore, be a saddle point shape. Note also the sudden drop in the value of the minor axis at $x=0.65$, implied by the Frankel and Metropolis solution (Fig. 7).

The calculations of Businaro and Gallone,[6] based on an expansion of the energy around an ellipsoid, with one harmonic, P_2, retained, exceed our values for ξ by 7.0%, 9.8%, 8.1%, and 11.1% at $x=0.9$, 0.8, 0.74, and 0.7, respectively. Similar calculations by Nossoff[7] ex-

TABLE IV. Radius vectors of saddle point shapes at $x=1.0$, 0.9, 0.8, 0.7, and 0.6.

θ	$x=1.0$	0.9	0.8	0.7	0.6
0°	1.000	1.227	1.476	1.785	2.140
10°	1.000	1.219	1.447	1.728	2.064
20°	1.000	1.182	1.363	1.576	1.828
30°	1.000	1.130	1.240	1.333	1.411
40°	1.000	1.072	1.097	1.071	1.020
50°	1.000	1.010	0.972	0.872	0.739
60°	1.000	0.956	0.878	0.747	0.588
70°	1.000	0.916	0.813	0.674	0.501
80°	1.000	0.892	0.777	0.637	0.471
90°	1.000	0.883	0.765	0.623	0.460

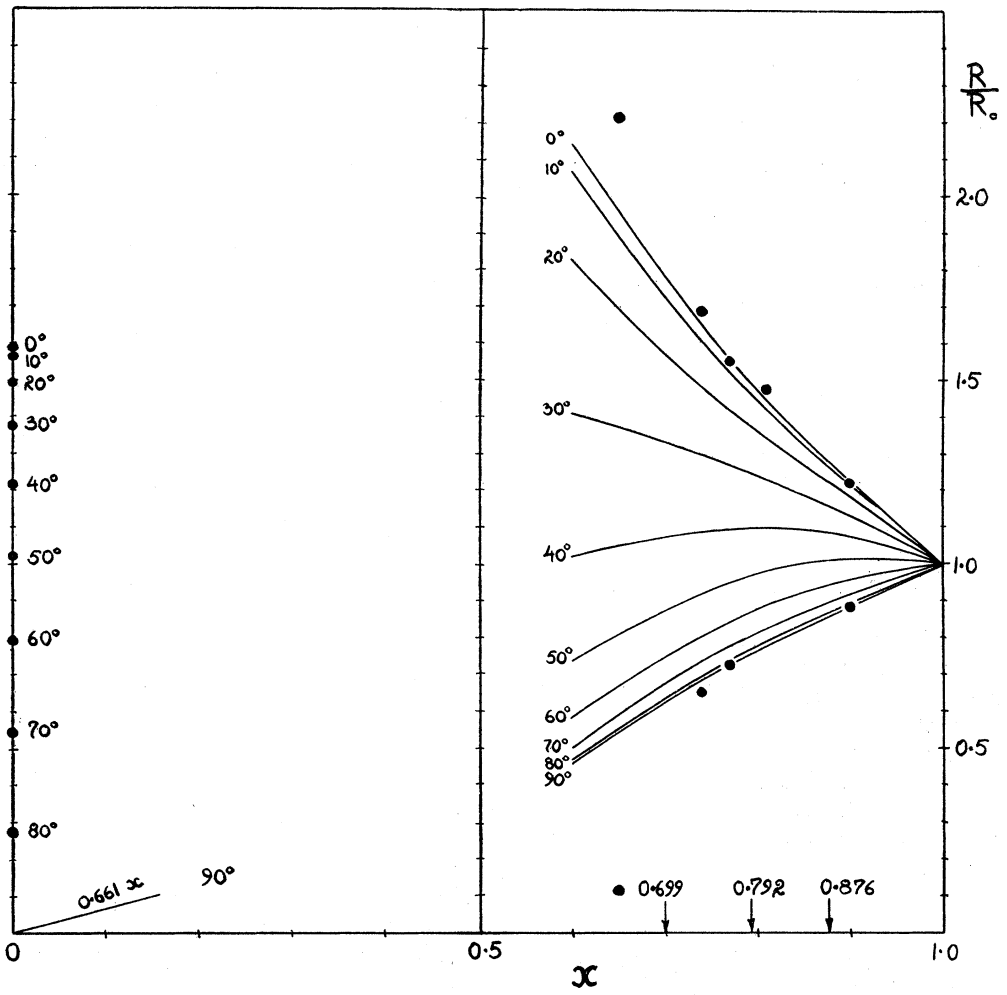

FIG. 7. Radius vectors of saddle point shapes as functions of x (in units of the radius R_0 of the original sphere), plotted at intervals of 10°. The curves pass through calculated points at the x values indicated by arrows and have the correct slope near $x=1$. The points on the left refer to the configuration of equal tangent spheres (the symmetric saddle point shape for $x=0$). The circled points give the major and minor axes calculated by Frankel and Metropolis.[4] (The value of the minor axis at $x=0.81$ is not given.)

ceed our ξ by amounts varying from 27% at $x=0.9$ to 46% at $x=0.65$

It may be noted that the simple formula $\xi=(98/135)\times(1-x)^3$, based on a lowest order expansion about a sphere [Eq. (11)], gives thresholds which are actually correct to within 10% down to $x=0.7$. This must be regarded as an accident, since the assumed expansion is certainly not valid for the very deformed shapes around $x=0.7$, as can be seen by noting that, on the one hand, the inclusion of the next term in $(1-x)^4$ gives a less satisfactory formula and, on the other, that the saddle point shapes calculated with the lowest order formula (11) provide a very poor representation of the correct shapes. (See Fig. 7.) As a rough, semi-empirical formula, however, the result

$$\xi=0.726(1-x)^3$$

should be useful in the range of values of x where the liquid drop model has been applied to the theory of nuclear fission.

ACKNOWLEDGMENTS

The major part of the work reported in this paper was carried out in 1951–53 during a stay at the Institute for Theoretical Physics in Copenhagen, as part of an investigation of the effects of charge redistribution on the theory of nuclear fission. I should like to thank Professor Niels Bohr for the hospitality of the Institute and several stimulating discussions. It is a pleasure to acknowledge the many discussions with my colleagues at the Institute.

I should also like to thank, in Copenhagen, Dr. Einar Andersen of the Geodaetisk Institut and Dr. Julie M. Vinter Hansen, director of the University Observatory, for facilities in connection with the numerical computations.

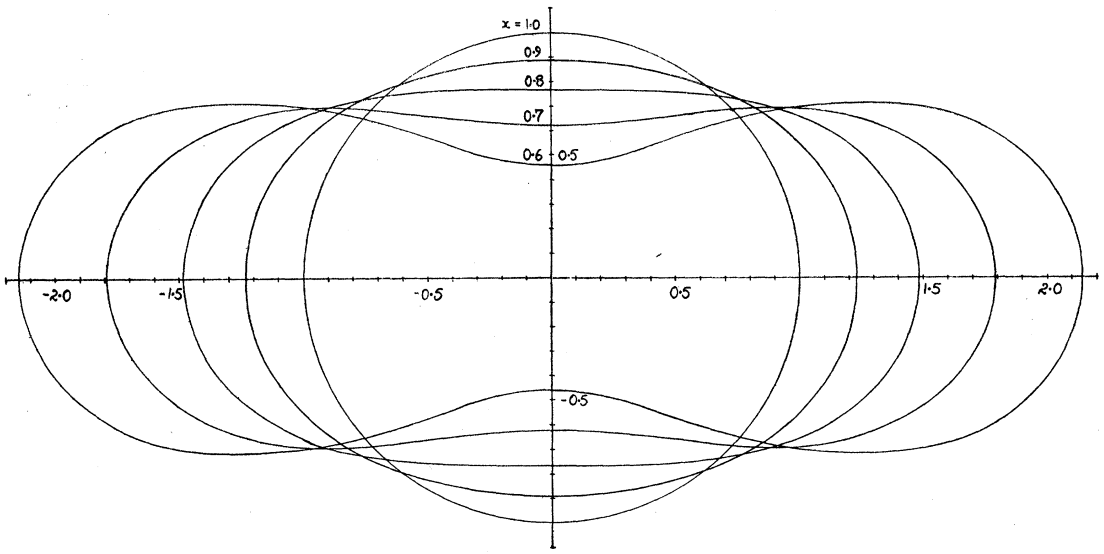

FIG. 8. Saddle point shapes for $x=1.0$, 0.9, 0.8, 0.7, and 0.6, obtained from the interpolation curves of Fig. 7.

The financial support of the Department for Scientific and Industrial Research in London, in the form of a Senior Research Award tenable during the period 1950–1953, is gratefully acknowledged.

The remainder of the work on this paper was done in Uppsala, and it is a pleasure to thank Professor I. Waller and Professor T. Svedberg for the hospitality of their Institutes, and the Swedish Atomkommitté for financial support.

APPENDIX

We shall give here an outline of the procedure used in deriving the coefficients in the expansions (18)–(21) and a summary of the results.

The first order expansion for v/v_0 in Eq. (18) is obtained by writing down the change in the surface potential as a sum of a term due to moving the surface in the field of the undistorted spheroid and a term which gives the potential on the spheroid due to the distortion (considered as an equivalent surface charge). For the potential of a surface charge on a spheroid, consult reference 9, especially page 206.

The expression (19) for B_c may be obtained by calculating the energy of the distortion (again considered as a surface charge) in the field of the spheroid. The fact that the surface potential on a spheroid is a *quadratic* function of ξ is responsible for the vanishing, by orthogonality of the P_n, of all coefficients a_n with $n>2$.

The derivation of the formula for κ/κ_0 was fairly involved. An intermediate step was the derivation of a general expression for the change $\delta\kappa$ in the total curvature of a surface of revolution associated with a distortion of the generating curve, specified by a normal displacement δn given as function of the length of arc s, i.e., $\delta n=\delta n(s)$. This formula reads:

$$\delta\kappa=-(R_1^{-2}+R_2^{-2})\delta n-\rho^{-1}\sin\theta\frac{d}{ds}(\delta n)-\frac{d^2}{ds^2}(\delta n),$$

where R_1, R_2 are the principal radii of curvature of the undistorted surface, ρ is the length of the cylindrical radius vector of the point in question and θ is the angle between this vector and the normal. Using the above expression in the case of a distortion specified in spheroidal coordinates, one obtains Eq. (20). The expression for B_s is obtained by using the relation

$$\delta A=\int_{\text{surface}}\kappa\delta n$$

for the change in area associated with a displacement δn. In this integral there appear expressions of the type

$$\int_{-1}^{1}d\xi(1-\xi^2/\eta_0)^{-r/2}P_n(\xi),$$

which give rise to the coefficients denoted by $D_n^{(r)}$ (see below). Special cases of such integrals have been considered by Bauer.[11]

The results of the steps just outlined are summarized below.

The functions $A(\xi)$, $A_n(\xi)$, $B(\xi)$, and $B_n(\xi)$ in Eqs. (18) and (20) were found to be given by the following expressions: Let

$$A=cH,\quad A_n=cH_n,\quad B=cM,\quad \text{and}\quad B_n=cM_n,$$

where

$$c=(1-\eta_0^{-2})^{\frac{1}{2}}.$$

[11] G. Bauer, Crelle's Journal **56**, 101 (1858).

Then

$$H=-\eta_0 Q_2 P_2,$$
$$H_2=\eta_0 Q_2/m-WP_2+T_2P_2,$$

and

$$H_{n>2}=-WP_n+T_nP_n,$$

where

$$W=\eta_0^2 w(Q_2'P_2-Q_0'),$$
$$T_n=3\eta_0 P_n(\eta_0)Q_n/m,$$
$$m=\eta_0^2-1,$$
$$w=(\eta_0^2-\xi^2)^{-1}.$$

Here P_n stands for the Legendre polynomial $P_n(\xi)$, with ξ as the argument, except where otherwise indicated. The Legendre polynomial of the second kind is denoted by Q_n (consult reference 8) and the argument is always η_0. The derivative $dQ_n/d\eta_0$ is denoted by Q_n'.

Similarly,

$$M=\tfrac{1}{10}(q-1-s),$$
$$M_{n>1}=\tfrac{1}{10}(RP_n+Sp_n+TP_n''-U_n),$$

where

$$s=m^{-\frac{1}{2}}\eta_0^2\sin^{-1}(1/\eta_0),$$
$$q=K(1+mw),$$
$$R=K[(-w/m)+(3-5\eta_0^2)w^2+3\eta_0^2 mw^3],$$
$$S=K(-w+3mw^2),$$
$$T=K(-1+mw),$$
$$K=\eta_0^2 w^{\frac{1}{2}}/m^{\frac{1}{2}}.$$

In the above, p_n stands for $\xi dP_n/d\xi$ and $P_n''=d^2P_n/d\xi^2$. Further, the coefficients U_n are given by

$$U_n=[\eta_0 m^{-\frac{3}{2}}D_n^{(-1)}+\eta_0^{-1}m^{-\frac{1}{2}}D_n^{(-3)}]/(n+\tfrac{1}{2}),$$

where the $D_n^{(r)}$ (which are functions of η_0) are the coefficients of $P_n(\xi)$ in the expansion of $(1-\xi^2/\eta_0^2)^{r/2}$ in Legendre polynomials:

$$(1-\xi^2/\eta_0^2)^{r/2}=\sum_0^\infty D_n^{(r)}P_n(\xi).$$

The $D_n^{(r)}$ can be calculated conveniently from the recurrence relation

$$D_{n+2}^{(r)}=\eta_0^2 L_n^{(r)}D_n^{(r)}-M_n^{(r)}D_n^{(r)}-N_n^{(r)}D_{n-2}^{(r)}, \quad (30)$$

where

$$L_n^{(r)}=\frac{(2n+3)(2n+5)}{(n+2)(n+r+3)},$$

$$M_n^{(r)}=\frac{(2n+3)(2n+5)n(n-r-2)}{(2n-1)(2n+1)(n+2)(n+r+3)}+\frac{(2n+5)(n+1)}{(2n+1)(n+2)},$$

$$N_n^{(r)}=\frac{(2n+3)(2n+5)(n-1)(n-r-2)}{(2n-3)(2n-1)(n+2)(n+r+3)}.$$

Further, for $r=-1$, we have

$$D_0^{(-1)}=\eta_0\sin^{-1}(1/\eta_0),$$
$$D_2^{(-1)}=(15/4)[(\eta_0^2-\tfrac{2}{3})D_0^{(-1)}-\eta_0(\eta_0^2-1)^{\frac{1}{2}}],$$

and for $r=-3$,

$$D_0^{(-3)}=\eta_0/(\eta_0^2-1)^{\frac{1}{2}},$$
$$D_2^{(-3)}=(15/2)[(\eta_0^2-\tfrac{1}{3})D_0^{(-3)}-\eta_0^3\sin^{-1}(1/\eta_0)].$$

TABLE V. Coefficients in the recurrence relation (30).

	$r=-1$			$r=-3$		
$n=$	2	4	6	2	4	6
L	63/16	143/36	255/64	63/8	143/24	85/16
M	15/8	247/126	697/352	9/2	65/21	119/44
N	21/16	143/140	2125/2112	63/8	143/56	2975/1584

Table V gives some of the coefficients $L_n^{(r)}$, $M_n^{(r)}$, $N_n^{(r)}$ explicitly.

The constants a, a_2, b, and b_n in Eqs. (19) and (21) are given by

$$a=c\eta_0 Q_0,$$
$$a_2=-c\eta_0 Q_2/m,$$
$$b=\tfrac{1}{2}c(1+s),$$
$$b_{n>1}=\tfrac{1}{2}cU_n.$$